Transition-metal Complexes of Pyrrole Pigments. Part 20.† Redox Behaviour of Chromium Complexes with Macrocyclic Tetrapyrroles

By **Yukito Murakami,* Yoshihisa Matsuda,** and **Sunao Yamada,** Department of Organic Synthesis, Faculty of Engineering, Kyushu University, Fukuoka 812, Japan

The redox chemistry of oxo(7,8,12,13-tetraethyl-2,3,17,18-tetramethylcorrolato)chromium(V), [Cr(O)(tetmc)], and the (5,10,15,20-tetraphenylporphinato)chromium(III) complexes, [Cr(tpp)X] (X = OMe or Cl), was investigated by means of cyclic voltammetry and controlled-potential electrolysis in the presence of tetrabutylammonium perchlorate at 25 ± 2 °C. Dichloromethane and *NN*-dimethylformamide were used as solvents for [Cr(O)(tetmc)] and [Cr(tpp)X] respectively. The compound [Cr(O)(tetmc)] underwent metal reduction more readily than [Mo(O)(tetmc)]. This was attributed to an extensive interaction between chromium d_{xy} and ligand orbitals which tends to reduce the *d*-electron density at the chromium site (nephelauxetic effect) and to raise the d_{xy} level. As for the tpp complexes, the first reduction took place at the ligand (tpp) site for [Cr(tpp)(OMe)] but at the metal site for [Cr(tpp)Cl]. The less ready reduction of the former complex at the metal site was attributed to effective covalent character of the Cr–OMe bond. Redox behaviour of the tpp complexes was discussed on the basis of the energy-level diagram of *d* orbitals under C_{4v} co-ordination symmetry and π-orbital interactions between chromium and tpp.

We have previously reported [1] the redox behaviour of oxo(7,8,12,13-tetraethyl-2,3,17,18-tetramethylcorrolato)-molybdenum(V), [Mo(O)(tetmc)], and the oxo(5,10,15,20-tetraphenylporphinato)molybdenum(V) complexes, [Mo(O)(tpp)X] (X = OMe, O_2CMe, or Cl). Oxidation and reduction potentials of the molybdenum nucleus for [Mo(O)(tpp)X] were very much dependent on the nature of the axial ligand X and consequently on the covalent character of the Mo^V–X bond; one-electron reduction becomes less ready as the covalent character increases and approaches the value of [Mo(O)(tetmc)] when X = OMe. The tpp complexes were much more resistant to oxidation of Mo^V than the tetmc complex.

Chromium, as another member of Group 6A, has been found to form complexes with tetraphenylporphine [2-4] and tetraethyltetramethylcorrole.[5] Thus, it is of interest to compare the redox behaviour of the chromium complexes with that of the corresponding molybdenum complexes. Furthermore, the chromium ion has been found to be involved in biological systems, although its function and structure have not yet been characterized. In connection with the enzymic functions of chromium, the redox chemistry of chromium complexes has attracted much attention recently and needs to be clarified as a result.

For these reasons, we have investigated the redox properties of the oxochromium(V) complex of 7,8,12,13-tetraethyl-2,3,17,18-tetramethylcorrole and the tervalent chromium complexes of 5,10,15,20-tetraphenylporphine, with either a methoxy- or a chloro-group as axial ligand, by cyclic voltammetry and controlled-potential electrolysis.

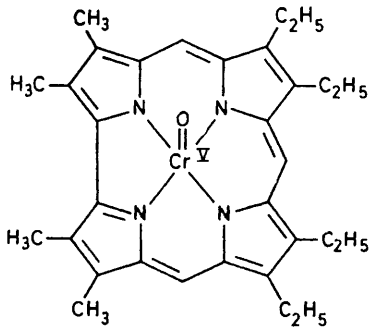

[Cr(O)(tetmc)]

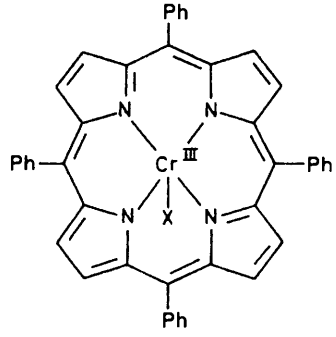

[Cr(tpp)X] X = OMe or Cl

EXPERIMENTAL

Materials.— Chloro(5,10,15,20-tetraphenylporphinato)-chromium(III), [Cr(tpp)Cl],[2,3] and methoxy(5,10,15,20-tetraphenylporphinato)chromium(III), [Cr(tpp)(OMe)],[4] were prepared by established procedures, and identified by electronic spectroscopy and elemental analyses. The preparation of oxo(7,8,12,13-tetraethyl-2,3,17,18-tetramethylcorrolato)chromium(V), [Cr(O)(tetmc)], has been described previously.[5] Dichloromethane was purified by the standard procedure [6] and kept over a molecular sieve (3A, Ishizu Pharmaceutical Co.). *NN*-Dimethylformamide of spectroscopic grade and tetrabutylammonium perchlorate

† Part 19, Y. Matsuda, S. Yamada, T. Goto, and Y. Murakami, *Bull. Chem. Soc. Jpn.*, in the press.

of polarographic grade were obtained from Dojindo Laboratories and Nakarai Chemicals respectively and used without further purification.

Spectroscopic Measurements.—Electronic absorption spectra covering the 350—800 nm range were recorded on a Union Giken SM-401 spectrophotometer. Electron spin resonance spectra were obtained on a JEOL JES-ME-3 *X*-band spectrometer equipped with a 100-kHz field modulation unit; a standard MgO–Mn^{II} sample calibrated with a n.m.r. magnetometer was employed for calibration of the magnetic field.

Electrochemical Measurements.—Cyclic voltammetry was carried out on a YANACO P-8 polarograph equipped with platinum wire of 0.5 mm diameter as working and auxiliary electrodes, the surface area of the former electrode being *ca.* 30 times smaller than that of the latter. A saturated calomel electrode (s.c.e.) served as a reference which was separated from a bulk electrolyte solution by a salt bridge prepared with benzylidene-D-sorbitol [7] and a dichloromethane solution of $[NBu_4][ClO_4]$. A dichloromethane solution containing a chromium complex (5.0×10^{-4}—6.0×10^{-4} mol dm^{-3}) and $[NBu_4][ClO_4]$ (5.0×10^{-2} mol dm^{-3}) was deaerated prior to each measurement and the inside of the cell was maintained under an argon atmosphere throughout each measurement. All the measurements were carried out at 25 ± 2 °C. The scan rate was varied in the range 5—500 mV s^{-1}. Half-wave potentials ($E_{\frac{1}{2}}$) and anodic (i_a) and cathodic (i_c) currents were evaluated by referring to the literature methods.[8]

Controlled-potential electrolysis was carried out in a three-electrode cell, modified for e.s.r. and electronic spectral measurements, with platinum wire of 0.5-mm diameter as working and auxiliary electrodes. The reference electrode was the same as that used for cyclic voltammetry. An applied potential between the working and auxiliary electrodes was kept constant with a conventional potentiostat and monitored with a Takeda Riken TR-6656 digital multimeter.

RESULTS

[Cr(O)(tetmc)].—The e.s.r. spectrum of [Cr(O)(tetmc)] measured in dichloromethane at room temperature is shown in Figure 1. The spectrum comprises nine intense lines at the centre and many weaker ones over a wider range. The central intense lines are assigned to the superhyperfine structure due to the interaction between four nitrogen nuclei co-ordinated to ^{50}Cr, ^{52}Cr, and ^{54}Cr ($I = 0$). The weaker signals are assigned to the superhyperfine structure caused by interactions between four nitrogen nuclei and a ^{53}Cr nucleus ($I = \frac{3}{2}$) as $I_z \pm \frac{3}{2}$ components while the range

TABLE 1

Spin-Hamiltonian and related parameters for [Cr(O)(tetmc)] and [Mo(O)(tetmc)] [a]

Complex	g	$10^4 A_{metal}/cm^{-1}$	$10^4 A_N/cm^{-1}$	Ref.
[Cr(O)(tetmc)]	1.987	19.3	3.3	This work
[Mo(O)(tetmc)]	1.967	41.8	2.3	*b*

[a] E.s.r. spectra of both complexes were measured in dichloromethane at room temperature. [b] Y. Murakami, Y. Matsuda, and S. Yamada, *Chem. Lett.*, 1977, 689.

of other components ($I_z = \pm\frac{1}{2}$) overlaps with the nine intense lines. The evaluated spin-Hamiltonian parameters are listed in Table 1, together with those for the corresponding molybdenum complex, [Mo(O)(tetmc)]. The intense signal was used to pursue the redox reactions of the complex.

Before conducting the controlled-potential electrolysis of [Cr(O)(tetmc)], the redox behaviour of the complex was examined by cyclic voltammetry. A typical cyclic voltammogram of [Cr(O)(tetmc)] in the range 1.5 to −0.7 V *vs.* s.c.e. is shown in Figure 2. Three cathodic peaks at 1.24, 0.57, and −0.37 V are coupled with anodic ones at 1.35, 0.68, and −0.27 V *vs.* s.c.e. respectively, as shown by I, II, and III_a in Figure 2; * each redox couple is ascribed to a one-electron transfer. The half-wave potentials ($E_{\frac{1}{2}}$) were evaluated from these redox couples (see Table 3). In order to characterize the complex species formed at each redox process, controlled-potential electrolysis was per-

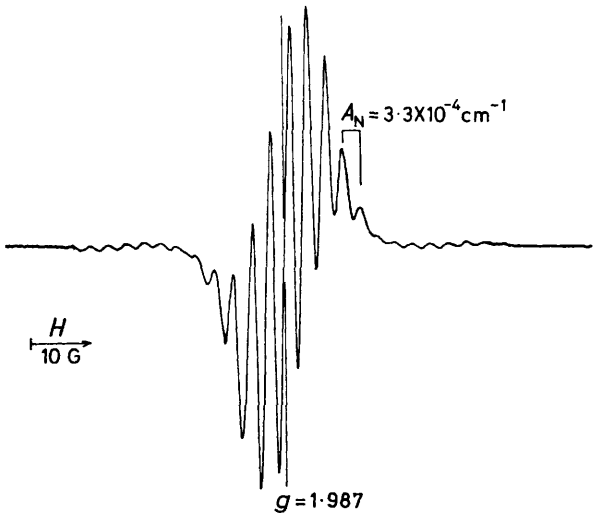

FIGURE 1 E.s.r. spectrum of [Cr(O)(tetmc)] in dichloromethane at room temperature

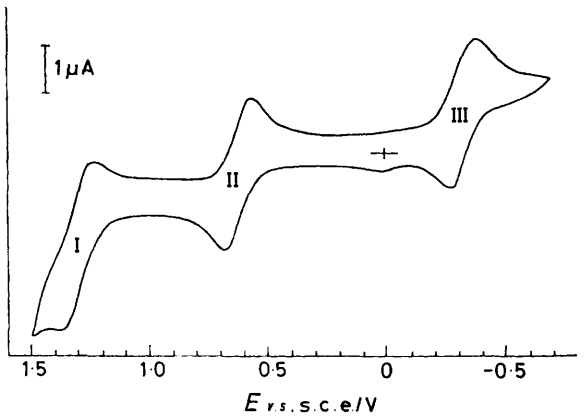

FIGURE 2 Cyclic voltammogram of [Cr(O)(tetmc)] (5.0×10^{-4} mol dm^{-3}) in dichloromethane containing 5.0×10^{-2} mol dm^{-3} $[NBu_4][ClO_4]$ at 25 °C: scan rate 100 mV s^{-1}

* The ratios of anodic to cathodic peak currents, $i_a : i_c$, were 1 : 1 and independent of scan rate (from 5 to 500 mV s^{-1}) for the three redox couples. Plots of i_p ($= i_a + i_c$) *vs.* $v^{\frac{1}{2}}$ (v is the scan rate in mV s^{-1}) were linear and potential separation between the anodic and cathodic peaks varied from 80 to 400 mV for the three redox couples, while $E_{\frac{1}{2}}$ values were constant within an accuracy of ±3%, regardless of scan rate variation. We, therefore, ascribe each redox process to reversible one-electron transfer without any coupled chemical reaction.

formed at 0.80 and −0.40 V *vs.* s.c.e. When a dichloromethane solution of [Cr(O)(tetmc)] (1.0×10^{-3} mol dm^{-3}) was electrochemically reduced at −0.40 V *vs.* s.c.e., the e.s.r. signal due to the parent complex disappeared completely and no other new signal was observed. Subsequent electrolytic reoxidation at 0 V *vs.* s.c.e. regenerated the parent signal, showing the reversible nature of the redox reaction. The controlled-potential reduction at −0.40 V *vs.* s.c.e. was also followed by electronic spectroscopy as shown in Figure 3, where clear isosbestic points are observed at 409, 463, 527, and 591 nm. The one-electron reduced species of [Cr(O)(tetmc)] shows intense visible bands, and the trend of spectral change along the progress of reduction resembles that observed for the reduction of [Mo(O)(tetmc)].[1] If the reduction were to occur at the ligand site, a new intense band in the lower-energy region would appear like that observed for the formation of a π-anion radical of [Zn(tpp)][9] and a monoanion radical of H_2tpp.[10] In the present reduction, however, such a band was not detected over the range 600—750 nm. On the basis of the electronic spectral features and the e.s.r. behaviour, we conclude that the one-electron reduction at peak III takes place at the

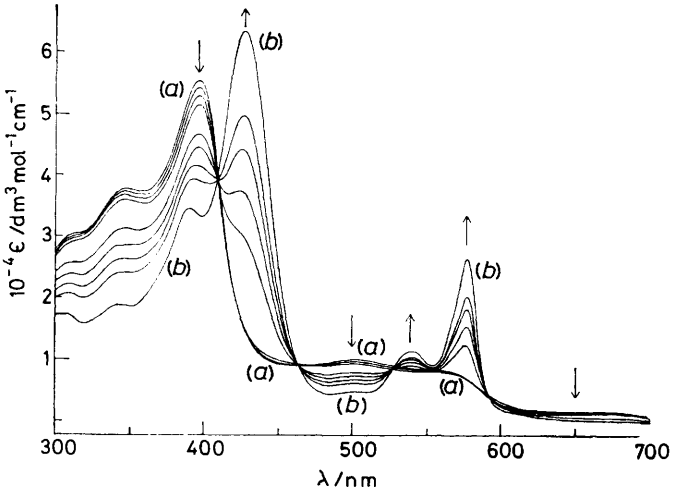

FIGURE 3 Electrochemical reduction of [Cr(O)(tetmc)] (3.1×10^{-5} mol dm^{-3}) at −0.40 V *vs.* s.c.e. in dichloromethane containing 5.0×10^{-2} mol dm^{-3} [NBu$_4$][ClO$_4$] at 25 °C: (*a*) [Cr^{V}(O)(tetmc)]; (*b*) one-electron reduced species. Trends of spectral change with time are shown by arrows

chromium site; Cr^{V}–Cr^{IV}. We also attempted chemical reduction of the complex with zinc–acetic acid, potassium iodide, and sodium benzophenone ketyl, but failed to reduce it quantitatively.

When the controlled-potential oxidation at 0.80 V and the subsequent re-reduction at 0 V *vs.* s.c.e. were performed, e.s.r. spectral changes, similar to those for the reduction at −0.40 V and the subsequent reoxidation at 0 V *vs.* s.c.e., were observed. The electronic spectral change in the course of electrolytic oxidation at 0.80 V *vs.* s.c.e. is shown in Figure 4, where isosbestic points are observed at 344, 362, 372, 436, 471, and 605 nm. A perfectly reversed spectral change was observed by re-reduction at 0 V *vs.* s.c.e. after the oxidation was completed at 0.80 V. Electronic spectral changes almost identical with those shown in Figure 4 were noted in the chemical oxidation and reduction processes by using anhydrous iron(III) chloride and potassium iodide respectively. A strong band due to [Cr(O)(tetmc)] observed at 398 nm remained in the same range and its intensity was not much reduced upon one-electron oxidation at 0.80 V *vs.* s.c.e. As for porphyrins, however, their cationic radical species show only one broad band over the

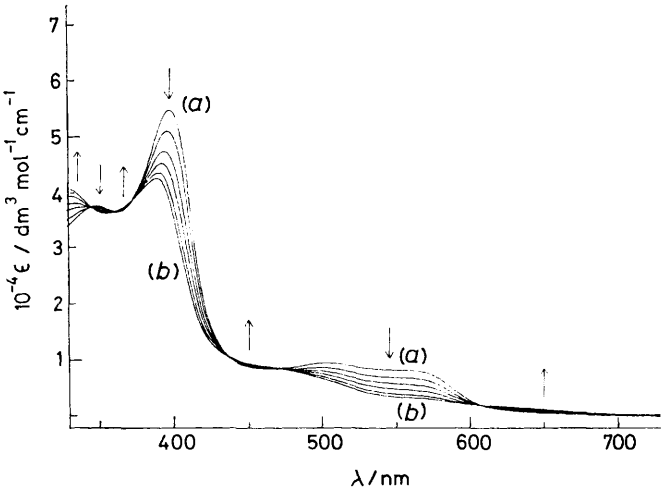

FIGURE 4 Electrochemical oxidation of [Cr(O)(tetmc)] (1.4×10^{-5} mol dm^{-3}) at 0.80 V *vs.* s.c.e. in dichloromethane containing 5.0×10^{-2} mol dm^{-3} [NBu$_4$][ClO$_4$] at 25 °C: (*a*) [Cr^{V}(O)(tetmc)]; (*b*) one-electron oxidized species. Trends of spectral change with time are shown by arrows

whole visible range and the intensity of the Soret band was markedly reduced.[11] These results indicate that the first one-electron removal from [Cr(O)(tetmc)] occurs at the metal site; peak II of Figure 2 is assigned to the redox couple Cr^{V}–Cr^{VI}. Electronic spectra for [Cr(O)(tetmc)] and its one-electron oxidized and reduced species are shown in

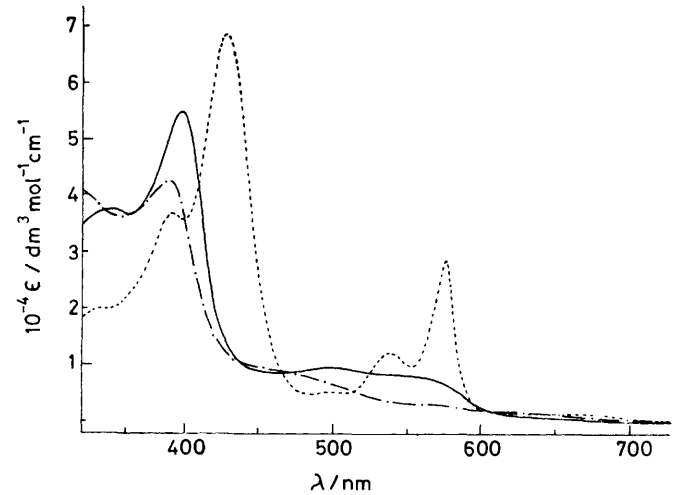

FIGURE 5 Electronic spectra of [Cr(O)(tetmc)] and its one-electron oxidized and reduced species in dichloromethane at 25 °C: [Cr^{V}(O)(tetmc)] (——); oxidized species (— · —) at 0.80 V *vs.* s.c.e. in the presence of [NBu$_4$][ClO$_4$] (5.0×10^{-2} mol dm^{-3}); reduced species (– – –) at −0.40 V *vs.* s.c.e. in the presence of [NBu$_4$][ClO$_4$] (5.0×10^{-2} mol dm^{-3})

Figure 5, and the corresponding spectral data obtained from electrochemical redox reactions are listed in Table 2. Since chromium(VI) has a d^0 configuration, no further oxidation takes place at the metal site beyond peak II in the anodic

region (Figure 2). We, therefore, assigned peak I to the oxidation of the corrole ligand. The redox behaviour of [Cr(O)(tetmc)] is shown in Scheme 1, and the evaluated half-wave potentials are listed in Table 3, together with those for [Mo(O)(tetmc)].

[Cr(tpp)X].—The complex [Cr(tpp)(OMe)] is a paramagnetic species having three unpaired *d* electrons in the solid state; $\mu_{eff.} = 3.933\ \mu_B$ at 296.4 K. However, no e.s.r. signal was observed in methanol, dichloromethane, or methanol–dichloromethane at room temperature. This seems attributable to the short spin–lattice relaxation time of the complex. *NN*-Dimethylformamide (dmf) dissolves both [Cr(tpp)(OMe)] and [Cr(tpp)Cl], but dichloromethane is not an efficient solvent for the latter. Thus, cyclic voltammetry was performed in dmf. A typical voltammogram of [Cr(tpp)(OMe)] over the range 0 to −2.0 V *vs.* s.c.e. is shown in Figure 6, where cathodic peaks at −1.21 and −1.81 V are coupled with anodic ones at −1.11 and −1.73 V *vs.* s.c.e. respectively. An anodic wave associated with the cathodic peak at −1.74 V *vs.* s.c.e. was not obvious at faster scan rates, but became so upon decreasing the scan rate; the redox couple was observed at −1.69 (cathodic) and −1.62 (anodic) V *vs.* s.c.e. for a scan rate of 5 mV s^{-1}. As a result, three one-electron redox couples were detected for [Cr(tpp)(OMe)] in the range 0 to −2.0 V *vs.* s.c.e. When pyridine was added to the dmf solution of [Cr(tpp)(OMe)], two new redox couples, centred at *ca.* −0.65 [IV in Figure 6(*b*)] and *ca.* −1.35 [V in Figure 6(*b*)] V *vs.* s.c.e., appeared. Their intensities increased with pyridine concentration while that of peak II decreased, as shown in Figure 6 [(*b*) and (*c*)]. In contrast to this marked current alteration for peak II, almost no intensity change was detected for peaks I and III. These results apparently indicate that peaks IV and V are caused by redox reactions of the chromium complexes co-ordinated to pyridine.

TABLE 2

Electronic spectra (band maxima/nm) for [Cr(O)(tetmc)] and its one-electron oxidized and reduced species in dichloromethane at 25 °C [a]

$[Cr^{V}(O)(tetmc)]$	$[Cr^{VI}(O)(tetmc)]^{+}$ [b]	$[Cr^{IV}(O)(tetmc)]^{-}$ [b]
398 (54.5)	386 (42.4)	343 (2.0)
499 (9.28)	485 (sh) (7.6)	391 (37)
570 (7.37)	612 (2.10)	428 (68)
721 (0.47)	662 (1.74)	500 (5)
		540 (13)
		577 (29)

[a] Molar absorption coefficients ($10^{-3}\ \epsilon$/dm^3 mol^{-1} cm^{-1}) are given in parentheses. [b] $[NBu_4][ClO_4]$ (5.0×10^{-2} mol dm^{-3}) added.

TABLE 3

Redox potentials for [Cr(O)(tetmc)] and [Mo(O)(tetmc)] in dichloromethane [a]

		Metal		Ligand		
Complex	θ_c/°C	$E_{\frac{1}{2}}^{ox.}$	$E_{\frac{1}{2}}^{red.}$	$E_{\frac{1}{2}}^{ox.}$	$E_{\frac{1}{2}}^{red.}$	Ref.
[Cr(O)(tetmc)]	25	0.63	−0.33	1.30	*b*	This work
[Mo(O)(tetmc)]	18	0.70	−0.72	1.3	*b*	*c*

[a] Concentration of complex, 5.0×10^{-4} mol dm^{-3}; $[NBu_4][ClO_4]$, 5.0×10^{-2} mol dm^{-3}. $E_{\frac{1}{2}}$ values are given in V *vs.* s.c.e. [b] A redox couple was not detected in a cathodic region up to −2.0 V *vs.* s.c.e. [c] Y. Murakami, Y. Matsuda, and S. Yamada, *Chem. Lett.*, 1977, 689.

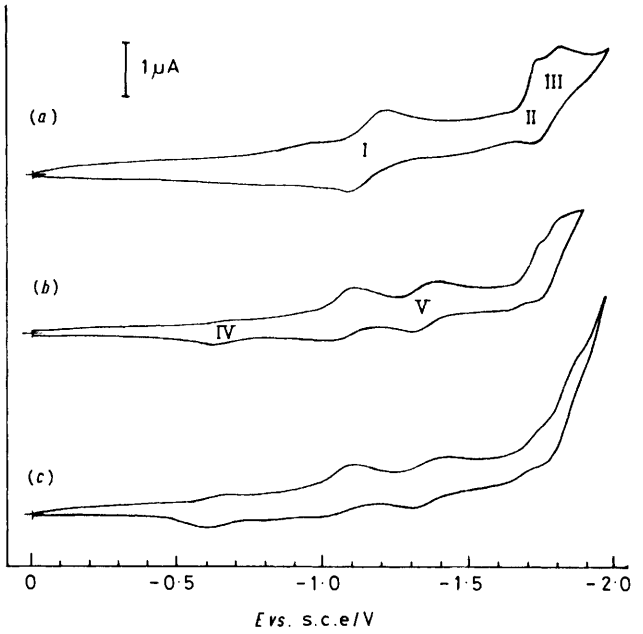

FIGURE 6 Cyclic voltammograms of [Cr(tpp)(OMe)] (5.0×10^{-4} mol dm^{-3}) in dmf containing 5.0×10^{-2} mol dm^{-3} $[NBu_4][ClO_4]$ at 25 °C in the presence of pyridine at various concentrations: (*a*) none; (*b*) 0.18 mol dm^{-3}; (*c*) 0.80 mol dm^{-3}; scan rate 50 mV s^{-1}

Cyclic voltammetry of [Cr(tpp)Cl] was also carried out, as shown in Figure 7, where three cathodic peaks of one-electron reduction at −0.90, −1.17, and −1.80 V are coupled with anodic ones at −0.75, −1.00, and −1.64 V *vs.* s.c.e. respectively. Assignments of redox reactions were made to these three couples by reference to the results obtained in dimethyl sulphoxide (dmso).[12] A cyclic voltammogram of [Cr(tpp)Cl] in pyridine showed only two redox couples centred at −0.62 and −1.41 V *vs.* s.c.e. at a scan rate of 100 mV s^{-1} in the range 0 to −2.0 V *vs.* s.c.e.; the former reduction takes place at the metal site as reported by Newton and Davis.[13]

Electronic spectra of [Cr(tpp)(OMe)] and [Cr(tpp)Cl] in pyridine resemble each other, and are different from those

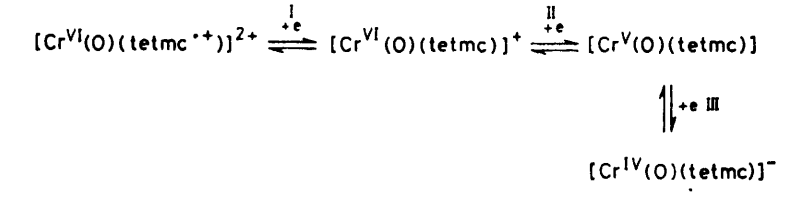

SCHEME 1 Roman numerals refer to the redox potential ranges shown in Figure 2

measured in dmf.* As a consequence, [Cr(tpp)X] is converted completely into the corresponding pyridine adduct in pyridine. Since only the peak II current (Figure 6) was subject to change in the presence of pyridine, peak II of [Cr(tpp)(OMe)] is attributed to the redox reaction Cr^{III}–Cr^{II}. On the basis of the above experimental results as well as the accompanying discussion, a plausible mode for redox

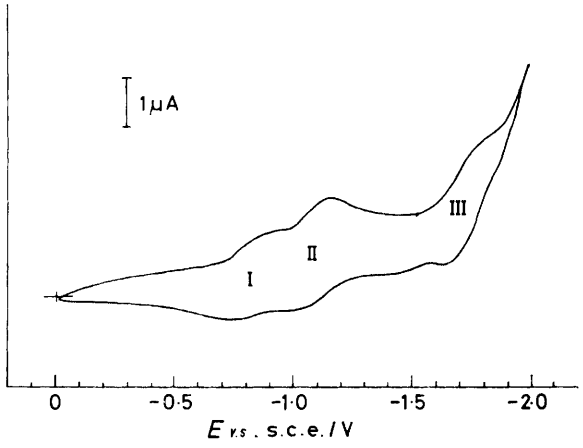

FIGURE 7 Cyclic voltammogram of [Cr(tpp)Cl] (6.0×10^{-4} mol dm^{-3}) in dmf containing 5.0×10^{-2} mol dm^{-3} $[NBu_4][ClO_4]$ at 24 °C: scan rate 100 mV s^{-1}

behaviour under the voltammetric conditions is shown in Scheme 2. The evaluated half-wave potentials are listed in Table 4 with assignments.

$$[Cr^{III}(tpp)(OMe)] \overset{I\ +e}{\rightleftharpoons} [Cr^{III}(tpp^{\cdot-})(OMe)]^{-} \overset{II\ +e}{\rightleftharpoons} [Cr^{II}(tpp^{\cdot-})(OMe)]^{2-}$$

$$\Big\| +e\ III$$

$$[Cr^{II}(tpp^{2-})(OMe)]^{3-}$$

$$[Cr^{III}(tpp)Cl)] \overset{I\ +e}{\rightleftharpoons} [Cr^{II}(tpp)] \overset{II\ +e}{\rightleftharpoons} [Cr^{II}(tpp^{\cdot-})]^{-} \overset{III\ +e}{\rightleftharpoons} [Cr^{II}(tpp^{2-})]^{2-}$$

SCHEME 2 Roman numerals refer to the redox potential ranges shown in Figures 6 and 7

DISCUSSION

[Cr(O)(tetmc)].—We have already confirmed the structural similarities between oxochromium(v) and oxomolybdenum(v) complexes of tetmc.[5] The only difference between the two complexes with respect to their electronic configurations is that one unpaired electron is placed in the $3d_{xy}$ orbital for [Cr(O)(tetmc)] and in the $4d_{xy}$ orbital for [Mo(O)(tetmc)]. It is interesting to note that the Cr^{V}–Cr^{VI} redox potential for [Cr(O)(tetmc)] is comparable to the Mo^{V}–Mo^{VI} potential for [Mo(O)(tetmc)]. From the ionization potentials of chromium and molybdenum,† it can be seen that the chromium ion has a greater electron–electron repulsion interaction in the d^2 configuration than the molybdenum ion. But, in the process of removing one d electron from these metals in the d^1 configuration, an appreciable difference in electron repulsion energy between the two metal ions cannot be expected. Thus, the energy of the $3d_{xy}$ orbital of [Cr(O)(tetmc)] must be raised through its interaction with ligand orbitals.

On the other hand, a large difference in metal reduction potential is noticed between the two complexes. The A_N value for [Cr(O)(tetmc)] is larger than that for [Mo(O)(tetmc)], showing a greater interaction between the chromium d_{xy} orbital and the σ and/or π orbitals of the corrolato-ligand. The potential difference for the IV→V and V→VI processes is 16.4 eV ‡ for chromium and 6.8 eV for molybdenum suggesting that [Cr(O)(tetmc)] is more resistant to reduction than [Mo(O)(tetmc)]. The contradictory result indicates that a strong covalent interaction exists between chromium and nitrogen-donor ligands.

TABLE 4

Redox potentials for [Cr(tpp)X] and [Mo(O)(tpp)X] (X = OMe or Cl) *

Compound	Solvent	θ_c/°C	Metal $E_{\frac{1}{2}}^{red.}$	Ligand $E_{\frac{1}{2}}^{red.}$ (1)	Ligand $E_{\frac{1}{2}}^{red.}$ (2)	Ref.
H_2tpp	CH_2Cl_2	26		−1.23	−1.56	1
[Cr(tpp)(OMe)]	dmf	25	−1.66	−1.16	−1.77	This work
[Cr(tpp)Cl]	dmf	24	−0.83	−1.09	−1.72	This work
[Cr(tpp)Cl]	dmso		−0.86	−1.23	−1.70	12
[Mo(O)(tpp)-(OMe)]	CH_2Cl_2	26	−0.74	−1.14	−1.49	1
[Mo(O)(tpp)Cl]	CH_2Cl_2	27	−0.06	−1.11	−1.50	1

* Concentration of complex, $(5.0–6.0) \times 10^{-4}$ mol dm^{-3}; $[NBu_4][ClO_4]$, 5.0×10^{-2} mol dm^{-3}. $E_{\frac{1}{2}}$ values are given in V *vs.* s.c.e.; within an accuracy of ±0.03 V.

Absorption bands in the 500—600 nm region intensify in proportion to the number of d electrons, from zero to two for [Cr(O)(tetmc)]. This strongly suggests that these bands are primarily attributed to metal (d)→ligand (π^*) charge-transfer transitions. A similar behaviour was observed for [Mo(O)(tetmc)].[1] The general

* Absorption band maxima (nm) of [Cr(tpp)(OMe)] (log ε) in dmf: 396 (4.44), 416 (sh) (4.67), 438 (5.36), 521 (3.76), 564 (4.06), and 601 (4.07); in pyridine: 371 (4.4), 409 (4.6), 456 (5.3), 526 (3.8), and 608 (4.1). Absorption band maxima (nm) of [Cr(tpp)Cl] (log ε) in dmf: 395 (4.50), 443 (5.30), 524 (3.68), 564 (4.03), and 601 (4.04); in pyridine: 369 (4.4), 408 (4.6), 457 (5.3), 529 (3.8), 572 (4.0), and 612 (4.1).

† Ionization potentials (eV) of chromium: III→IV, 49.6; IV→V, 73; V→VI, 90.6. Ionization potentials (eV) of molybdenum: III→IV, 46.4; IV→V, 61.2; V→VI, 68. The data are cited from C. E. Moore. 'Atomic Energy Levels,' Circular of the National Bureau of Standards 467, Washington, D.C., 1952, vol. 2 and 1958, vol. 3.

‡ Throughout this paper: 1 eV ≈ 1.60×10^{-19} J.

feature of Soret-type bands for +6, +5, and +4 valency states of chromium, however, is somewhat different from that for Mo. The one-electron reduced species of [Mo(O)(tetmc)] shows a strong and narrow Soret-type band compared with those of the parent and the one-electron oxidized species.[1] In spite of variation of the number of *d* electrons from zero to two, the intensity of Soret-type bands does not undergo any significant change as for [Cr(O)(tetmc)]. Furthermore, the Soret-type bands for [Cr(O)(tetmc)] species at all the metal valency states concerned here are broader and somewhat lower in intensity than those for the corresponding molybdenum complexes. This is probably attributable to the lower molecular symmetry of [Cr(O)(tetmc)] compared with [Mo(O)(tetmc)].

Very recently, Groves and Kruper [14] indicated the existence of an oxo(porphinato)chromium(v) complex as a detectable reaction intermediate in solution by means of i.r. and magnetic measurements. This complex was, however, generated only by the reaction of an active oxygenation reagent, iodosylbenzene, with [Cr(tpp)Cl]. An oxochromium(v) complex was readily obtained by using another macrocyclic tetrapyrrole, tetmc.[5] This must be due to the fact that the corrole skeleton has a much smaller cavity size for incorporation of a metal ion relative to the porphyrin skeleton and the π basicity of the former is higher than the latter, both structural aspects of tetmc favouring the chromium(v) state.

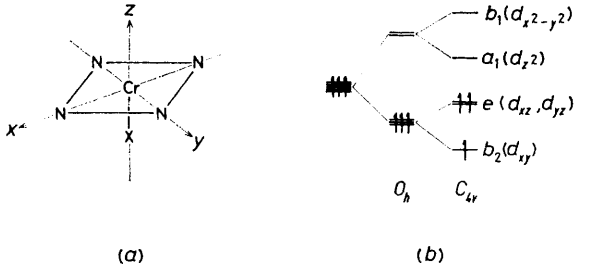

FIGURE 8 Energy-level diagram for chromium(III) *d* orbitals under C_{4v} symmetry: (*a*) schematic representation of co-ordinate axes; (*b*) energy-level correlation between O_h and C_{4v} co-ordination symmetries

[Cr(tpp)X].—The energy-level diagram of *d* orbitals for [Cr(tpp)X] under C_{4v} co-ordination symmetry is shown in Figure 8. The lowest level is most likely to be due to the non-bonding d_{xy} orbital (b_2).

As reported previously,[1] the Mo–OMe bond in [Mo(O)(tpp)(OMe)] has appreciable covalent character while the Mo–Cl bond in [Mo(O)(tpp)Cl] is rather ionic. Such covalent character gives rise to a cathodic shift of the molybdenum reduction potential relative to the corresponding potential for the latter complex (Table 4). In a similar manner, the Cr–OMe bond in [Cr(tpp)(OMe)] must have a considerable covalent character which tends to increase the electron density at the chromium atom so that all *d*-orbital levels are forced to be raised slightly. Meanwhile, the a_1 level is raised just above the tpp π* level. This effect on *d* orbitals gives rise to the $d\pi(e)$–$p\pi^*$ interaction which causes the π* level to rise, while such an effect is not expected for [Cr(tpp)Cl]. The first reduction of [Cr(tpp)(OMe)] takes place at the ligand (tpp) site and its π* orbital accepts one electron. The extent of $d\pi(e)$–$p\pi^*$ interaction must be responsible for the difference in the first ligand-reduction potential between [Cr(tpp)(OMe)] and [Cr(tpp)Cl] as measured in dmf. In the second reduction process, an additional electron is most likely added to one of the three lower *d* orbitals (b_2 and *e*) since the energy separation between *e* and a_1 levels would be much greater than the inter-electronic repulsion energy. In such a case, the axial co-ordinate bond must be retained in the course of reduction. The two-electron reduced species of [Cr(tpp)(OMe)] may have a five-co-ordinate structure with an intermediate spin state ($S = 1$) like that observed for $[Cr^{II}(tpp)(py)_2]$ (py = pyridine) with six-co-ordination.[15] The second reduction to $[Cr^{II}(tpp^{\cdot-})(OMe)]^{2-}$ increases the electron density at the chromium *d* orbitals and the $d\pi(e)$ level is raised as a result. Such an effect tends to increase the $d\pi(e)$–$p\pi^*$ interaction which further increases the electron density at the metal atom and concomitantly the π-antibonding level of tpp is raised. As a result, the third reduction to afford $[Cr^{II}(tpp^{2-})(OMe)]^{3-}$ takes place in a higher cathodic region relative to the reduction of $[Cr^{II}(tpp^{\cdot-})]$ derived from [Cr(tpp)Cl].

The Cr–Cl bond in [Cr(tpp)Cl] seems to have ionic character like the Mo–Cl bond of [Mo(O)(tpp)Cl].[1] Consequently, the a_1 level is not much perturbed by axial co-ordination so that an electron added to the chromium complex during the first reduction process must occupy the d_{z^2} orbital; the metal reduction potential is shifted toward the anodic direction by *ca.* 0.8 V relative to that of the methoxy-complex. Although Basolo and co-workers [16] reported the formation of six-co-ordinated species, [Cr(tpp)Cl(dmf)] and [Cr(tpp)Cl(dmso)], the axial ligation of dmf or dmso is not strong enough to perturb the a_1 level significantly. The first reduction process introduces one electron into the d_{z^2} orbital which has antibonding character to the axial co-ordination. Such reduction results in Cr–Cl bond cleavage to afford $[Cr^{II}(tpp)]$ with a high-spin d^4 configuration as confirmed by Cheung *et al.*[12] Both second and third reductions take place at the ligand site, each donating one electron to the porphyrin π* orbital. The ligand reduction processes for the molybdenum complexes are as follows: [1] $[Mo^{IV}(O)(tpp)] \rightarrow [Mo^{IV}(O)(tpp^{\cdot-})]^-$ and $[Mo^{IV}(O)(tpp^{\cdot-})]^- \rightarrow [Mo^{IV}(O)(tpp^{2-})]^{2-}$. For these cases, the d_{xz} and d_{yz} orbitals are vacant and thus can accept electrons from the tpp π* orbitals through $d\pi$–$p\pi^*$ interaction. The electron density of the π-antibonding orbitals is lowered by $d\pi$–$p\pi^*$(tpp) and $d\pi$–$p\pi^*$(oxo) interactions as a consequence. Such interactions cannot be verified for the present chromium complexes.

[0/1188 *Received*, 28*th July*, 1980]

REFERENCES

[1] Y. Matsuda, S. Yamada, and Y. Murakami, *Inorg. Chem.*, submitted for publication.
[2] A. D. Adler, F. R. Longo, F. Kampas, and J. Kim, *J. Inorg. Nucl. Chem.*, 1970, **32**, 2443.

[3] J. A. Shelnutt, D. C. O'Shea, N.-T. Yu, L. D. Cheung, and R. H. Felton, *J. Chem. Phys.*, 1976, **64**, 1156.
[4] E. B. Fleischer and T. S. Srivastava, *Inorg. Chim. Acta*, 1971, **5**, 151.
[5] Y. Matsuda, S. Yamada, and Y. Murakami, *Inorg. Chim. Acta*, 1980, **44**, L309.
[6] J. A. Riddick and W. B. Bunger, 'Organic Solvents,' Wiley–Interscience, New York, 1970.
[7] F. Endo, *Yakugaku Zasshi*, 1959, **79**, 595.
[8] R. N. Adams, 'Electrochemistry at Solid Electrodes,' Marcel Dekker, New York, 1969, pp. 143—162.
[9] G. L. Closs and L. E. Closs, *J. Am. Chem. Soc.*, 1963, **85**, 818.
[10] G. Peychal-Heiling and G. S. Wilson, *Anal. Chem.*, 1971, **43**, 550.
[11] See for example, A. Wolberg and J. Manassen, *J. Am. Chem. Soc.*, 1970, **92**, 2982.
[12] S. K. Cheung, C. J. Grimes, J. Wong, and C. A. Reed, *J. Am. Chem. Soc.*, 1976, **98**, 5028.
[13] C. M. Newton and D. G. Davis, *J. Magn. Reson.*, 1975, **20**, 446.
[14] J. T. Groves and W. J. Kruper, jun., *J. Am. Chem. Soc.*, 1979, **101**, 7613.
[15] W. R. Scheidt, A. C. Brinegar, J. F. Kirner, and C. A. Reed, *Inorg. Chem.*, 1979, **18**, 3610.
[16] D. A. Summerville, R. D. Jones, B. M. Hoffman, and F. Basolo, *J. Am. Chem. Soc.*, 1977, **99**, 8195.